

Stokes Flow about a Slip Arbitrary-Shaped Particle

A. Sellier

Abstract: A new approach is proposed to accurately compute at a reasonable cpu time cost the hydrodynamic net force and net torque exerted on a slip and arbitrarily-shaped solid particle experiencing a prescribed slow rigid-body migration in a quiescent Newtonian liquid. The advocated method appeals to a boundary formulation which makes it possible to reduce the task to the treatment of a relevant regularized boundary-integral equation on the particle slipping surface. This integral equation is numerically inverted by implementing a boundary element collocation method. In addition to benchmark tests against analytical and numerical results available in the literature, numerical results for volume-equivalent ellipsoids and open torus are given and discussed.

Keywords: Slip particle, Stokes flow, Navier slip condition, Boundary-integral equation, Boundary Element Method.

1 Introduction

Many basic applications nowadays involve flows of a Newtonian fluid (liquid or rarefied gas in the continuum regime) with uniform viscosity μ and density ρ about migrating solid particles. For dilute and unbounded suspensions it is possible to restrict attention to the case of a flow with typical velocity magnitude V about a single particle with length scale a . Sometimes it turns out that $Re = \rho Va/\mu \ll 1$ (i. e. negligible inertial effects) and the flow about the particle is then taken to be a steady creeping flow governed by the linear Stokes equations, a suitable far-field behavior and additional boundary conditions on the particle's surface S . A large body of literature (see, for instance, Happel and Brenner (1991); Kim and Karrila (1991)) has been devoted to the usual case of a no-slip condition on S .

However, in some cases (rarefied gas or liquid near a solid hydrophobic or lyophobic surface) the flow is allowed to flow over the particle surface and one then usually prescribes on S the so-called Navier (1823) slip condition. This slip condition, now experimentally well supported (Churaev, Sobolev, and Somov (1994); Baudry, Charlaix, Tonck, and Mazuyer (2001)) takes for a particle with translational veloc-

ity \mathbf{U} and angular velocity Ω the form given by equation (3) where the occurring slip length $\lambda \geq 0$ characterizes the surface ability to let the flow slip over it. Within this framework, Basset (1961) analytically obtained the flow about a slip sphere with radius a migrating in a quiescent liquid. He found the net hydrodynamic force \mathbf{F} and torque (about the sphere center) \mathbf{L} to be given by (11) and (14), *respectively*. Unfortunately, for a slip non-spherical particle there is no such analytical solution and another treatment is required. Several works have thus proposed in the last decade quite different approaches for axisymmetric or weakly non-axisymmetric slip particles. One can actually distinguish two cases:

(i) The case of a nearly-spherical slip particle for which the departure of the particle's surface from a sphere is quantified by a small positive and dimensionless parameter ε . In that case one then asymptotically builds the solution versus ε up to the second-order. In this direction one can cite Palaniappan (1994) and Ramkissoon (1997) further corrected by Senchenko and Keh (2006) and also, more recently, Chang and Keh (2009).

(ii) The case of a slip particle with axis of revolution. The first paper in this direction seemingly is Williams (1987a) which gives the force and the drag exerted on a closed torus experiencing a translation and/or a rotation parallel with its axis of revolution. The investigation uses the toroidal coordinates (see, for instance, Williams (1987b)). The results for the torque were later numerically confirmed by Loyalka (1996) by employing the boundary-integral equation introduced in Loyalka and Griffin (1994) to solve the boundary-value problem satisfied by the *harmonic* velocity component of the rotational fluid motion about a slip and axisymmetric particle rotating parallel with its axis of revolution. Note that Loyalka and Griffin (1994) also examines both theoretically (using spheroidal coordinates; see also for details Williams and Loyalka (1991)) and numerically (solving the previously-mentioned boundary-integral equation) the *rotation* of a slip spheroid (either prolate or oblate ones) about its axis of revolution. This case of the rotating spheroid has been also recently treated by the asymptotic method in Chang and Keh (2009). Results for a spheroid *translating* parallel with its axis of revolution have been obtained by Keh and Huang (2004) putting so-called Sampson spherical singularities inside the spheroid and also by Deo and Datta (1996) (for a prolate spheroid) and Keh and Chang (2008) by building a semi-separable general solution for the stream function. Finally, the extension of Keh and Huang (2004) to the case of the *translation* of a slip axisymmetric particle normal to its axis of revolution has been recently achieved in Chang and Keh (2011) with numerical results given for a spheroid.

In summary, there is still the need to propose a new method to efficiently cope with the case of a slip and arbitrarily-shaped particle. The aim of the present work is to introduce such a procedure. More precisely, the paper is organized as follows. The

governing assumptions and equations are given together with the analytical solution for a sphere in §2. A new boundary formulation and a relevant boundary-integral equation on the particle surface are examined in §3. The numerical implementation and both benchmark tests and numerical results are presented in §4. Finally, a few concluding remarks in §5 close the paper.

2 Addressed problem and analytical solution for a slip spherical particle

This section presents the addressed problem for a solid and arbitrarily-shaped slip particle. For further comparisons purposes, it also gives the available analytical solution for a slip spherical particle.

2.1 Governing equations and challenging issues

As illustrated in Fig. 1, we consider a solid particle \mathcal{P} , with smooth surface S and center of volume O , immersed in a quiescent and unbounded Newtonian liquid with uniform density ρ and viscosity μ .

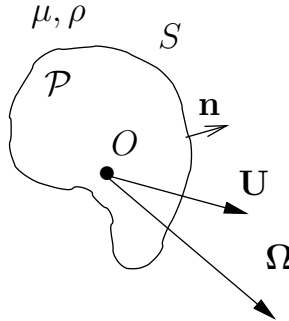


Figure 1: A solid slip particle \mathcal{P} experiencing a prescribed rigid-body migration with translational velocity \mathbf{U} and angular velocity $\mathbf{\Omega}$.

For convenience we shall use Cartesian coordinates (O, x_1, x_2, x_3) with the notations $\mathbf{x} = \mathbf{O}\mathbf{M}$, $x_i = \mathbf{x} \cdot \mathbf{e}_i$ for $i = 1, 2, 3$ and $r = |\mathbf{x}| = \{x_1^2 + x_2^2 + x_3^2\}^{1/2}$. With respect to a given Laboratory frame, the particle experiences a prescribed rigid-body migration with translational velocity \mathbf{U} (here the the velocity of its attached point O) and angular velocity $\mathbf{\Omega}$. Moreover, the particle has typical length scale a and the flow about it has pressure field p and velocity field \mathbf{u} with typical magnitude V . Assuming that $\text{Re} = \rho Va/\mu \ll 1$ (case for instance of micro-sized particles and/or slow migration) makes it possible to neglect all inertial effects. Under this assumption the flow (\mathbf{u}, p) fulfills in the liquid domain \mathcal{D} the steady Stokes equations (see

Happel and Brenner (1991)) and far-field behaviour

$$\mu \nabla^2 \mathbf{u} = \nabla p \quad \text{and} \quad \nabla \cdot \mathbf{u} = 0 \quad \text{in } \mathcal{D}, \tag{1}$$

$$(\mathbf{u}, p) \rightarrow (\mathbf{0}, 0) \quad \text{as } |\mathbf{x}| \rightarrow \infty. \tag{2}$$

One must of course supplement (1)-(2) with relevant boundary conditions on the smooth slip particle surface S having unit normal \mathbf{n} directed into the liquid. Usually one requires a no-slip condition but here we deal with a slip particle: the flow (\mathbf{u}, p) , with stress tensor $\boldsymbol{\sigma}$, is allowed to slip over the surface S . This is modeled for the present work by adopting the following widely-employed and so-called Navier (1823) slip condition

$$\mathbf{u} = \mathbf{U} + \boldsymbol{\Omega} \wedge \mathbf{OM} + \lambda \{ \boldsymbol{\sigma} \cdot \mathbf{n} - (\mathbf{n} \cdot \boldsymbol{\sigma} \cdot \mathbf{n}) \mathbf{n} \} / \mu \quad \text{on } S \tag{3}$$

where $\lambda \geq 0$ designates the slip length. In practice, λ depends upon the nature of the particle surface (think, for instance, about hydrophobic surfaces). Although one might consider in some applications slip surfaces with a non-uniform slip length, we assume for the present work that λ is constant over the particle surface. Note that the usual no-slip boundary condition is retrieved for $\lambda = 0$.

For a given particle with prescribed rigid-body motion $(\mathbf{U}, \boldsymbol{\Omega})$ and slip length λ one obtains the flow (\mathbf{u}, p) and the surface traction $\mathbf{f} = \boldsymbol{\sigma} \cdot \mathbf{n}$ it exerts on the slip particle surface by solving (1)-(3). As a result, it is subsequently possible to evaluate the net hydrodynamic force \mathbf{F} and torque \mathbf{L} (about the attached point O) experienced by the moving particle and given by

$$\mathbf{F} = \int_S \boldsymbol{\sigma} \cdot \mathbf{n} dS, \quad \mathbf{L} = \int_S \mathbf{x} \wedge \boldsymbol{\sigma} \cdot \mathbf{n} dS. \tag{4}$$

By linearity of the problem (1)-(3), these quantities depend upon the rigid-body motion $(\mathbf{U}, \boldsymbol{\Omega})$ in the following manner

$$\mathbf{F} = -\mu \{ \mathbf{A} \cdot \mathbf{U} + \mathbf{B} \cdot \boldsymbol{\Omega} \}, \quad \mathbf{L} = -\mu \{ \mathbf{C} \cdot \mathbf{U} + \mathbf{D} \cdot \boldsymbol{\Omega} \} \tag{5}$$

where $\mathbf{A}, \mathbf{B}, \mathbf{C}$ and \mathbf{D} are second-rank resistance tensors which depend upon the particle geometry and slip length λ . Whatever the particle's surface shape and slip length it is possible to establish that both tensors \mathbf{A} and \mathbf{D} are symmetric whereas tensors \mathbf{C} and \mathbf{B} are transposed (the proof, let to the reader, appeals to the reciprocal identity). As a consequence, one can reduce the determination of the above tensors Cartesian components to the computation of at the most 21 coefficients.

As mentioned in the introduction, getting the flow (\mathbf{u}, p) , the surface traction \mathbf{f} and the vectors \mathbf{F} and \mathbf{L} for arbitrary particle shape, slip length λ and rigid-body motion $(\mathbf{U}, \boldsymbol{\Omega})$ is a very challenging issue which has, to the author's very best knowledge, not yet received a general treatment.

2.2 Analytical solution for a slip spherical particle

When the flow is not allowed to slip over the particle surface ($\lambda = 0$) one ends up with the widely-investigated (see, among other references, Happel and Brenner (1991); Kim and Karrila (1991)) problem of the Stokes flow about a migrating solid particle with the usual no-slip condition $\mathbf{u} = \mathbf{U} + \boldsymbol{\Omega} \wedge \mathbf{OM}$ on the particle surface. In that case it is possible to analytically solve Jeffery (1922); Lamb (1932) the problem for a translating and/or rotating ellipsoidal particle with arbitrary semi-axis (i. e. not only for spheroids). Amazingly, no such analytical solutions are available for a slip ellipsoid or even a slip spheroid. Actually, for $\lambda > 0$ analytical results have only been obtained for a slip spherical particle with center O and radius a . Since useful when benchmarking the boundary approach proposed in the present paper, those results are briefly given below by successively distinguishing (by linearty) two cases:

(i) *The translating sphere.* When the sphere translates, without rotating, at the velocity \mathbf{U} the Stokes flow (\mathbf{u}, p) about the particle is obtained by superposing a Stokeslet and a potential dipole located at the sphere center and having unknown strength \mathbf{s} and \mathbf{e} , respectively. Hence,

$$\mathbf{u} = \frac{\mathbf{s}}{r} + \frac{(\mathbf{s} \cdot \mathbf{x})\mathbf{x}}{r^3} + 3\frac{(\mathbf{e} \cdot \mathbf{x})\mathbf{x}}{r^5} - \frac{\mathbf{e}}{r^3} \quad \text{for } r = |\mathbf{x}| > a, \quad (6)$$

$$p = 2\mu\left(\frac{\mathbf{s} \cdot \mathbf{x}}{r^3}\right) \quad \text{for } r = |\mathbf{x}| > a. \quad (7)$$

Of course (see, for instance, Kim and Karrila (1991); Pozrikidis (1992)) both (1) and (2) are satisfied whatever (\mathbf{s}, \mathbf{e}) . Imposing the Navier boundary condition (3) further easily yields

$$a^3\mathbf{s} - a\mathbf{e} = a^4\mathbf{U} + 6\lambda\mathbf{e}, \quad a^3\mathbf{s} + 3a\mathbf{e} = -6\lambda\mathbf{e}. \quad (8)$$

As a consequence,

$$\mathbf{s} = \frac{3a(1 + 2\lambda/a)\mathbf{U}}{4(1 + 3\lambda/a)}, \quad \mathbf{e} = -\frac{a^3\mathbf{U}}{4(1 + 3\lambda/a)}. \quad (9)$$

Accordingly, the surface traction $\mathbf{f} = \boldsymbol{\sigma} \cdot \mathbf{n}$, the net force \mathbf{F} and the net torque \mathbf{L} exerted on the translating slip sphere read

$$\mathbf{f} = -\frac{3\mu a^3}{2(1 + 3\lambda/a)} \left\{ \mathbf{U} + 6\lambda \frac{(\mathbf{U} \cdot \mathbf{x})\mathbf{x}}{a^3} \right\}, \quad (10)$$

$$\mathbf{F} = -6\pi\mu a \left[\frac{1 + 2\lambda/a}{1 + 3\lambda/a} \right] \mathbf{U}, \quad \mathbf{L} = \mathbf{0}. \quad (11)$$

(ii) *The rotating sphere.* When the sphere rotates, without translating, at the velocity Ω one gets the flow by placing this time at the sphere center a rotlet with unknown strength γ . In other words,

$$\mathbf{u} = \frac{\gamma \wedge \mathbf{x}}{r^3} \text{ and } p = 0 \text{ for } r = |\mathbf{x}| > a. \tag{12}$$

The flow (\mathbf{u}, p) given by (12) fulfills (1)-(2). Exploiting the Navier boundary condition (3) gives

$$\gamma = \frac{a^3 \Omega}{1 + 3\lambda/a}. \tag{13}$$

Therefore, the resulting surface force $\mathbf{f} = \boldsymbol{\sigma} \cdot \mathbf{n}$, net force \mathbf{F} and net torque \mathbf{L} are

$$\mathbf{f} = -\frac{3\mu[\Omega \wedge \mathbf{x}]}{a(1 + 3\lambda/a)}, \mathbf{F} = \mathbf{0}, \mathbf{L} = -\frac{8\pi\mu a^3 \Omega}{1 + 3\lambda/a}. \tag{14}$$

3 Advocated boundary approach

For a non-spherical slip particle a numerical treatment is needed to accurately solve the problem (1)-(3). This is achieved by implementing a suitable boundary approach presented in this key section.

3.1 Key velocity integral representation

For convenience, we adopt henceforth the usual tensor summation convention with, for instance, $\mathbf{x} = x_i \mathbf{e}_i$ and $\mathbf{n} = n_i \mathbf{e}_i$. As shown by (1)-(2), the velocity field \mathbf{u} about the particle is a steady creeping flow field vanishing far from the particle. Consequently (see Pozrikidis (1992)), the vector \mathbf{u} admits in the entire liquid domain \mathcal{D} the following key integral representation

$$\mathbf{u}(\mathbf{x}) \cdot \mathbf{e}_j = -\frac{1}{8\pi} \int_S \left\{ \left[\frac{\mathbf{e}_i \cdot \boldsymbol{\sigma} \cdot \mathbf{n}}{\mu} \right](\mathbf{y}) G_{ij}(\mathbf{y}, \mathbf{x}) - [\mathbf{u}(\mathbf{y}) \cdot \mathbf{e}_i] T_{ijk}(\mathbf{y}, \mathbf{x}) n_k(\mathbf{y}) \right\} dS(\mathbf{y}) \text{ for } \mathbf{x} \text{ in } \mathcal{D} \tag{15}$$

with, denoting by δ the Kronecker delta symbol, the definitions

$$G_{ij}(\mathbf{x}, \mathbf{y}) = \frac{\delta_{ij}}{|\mathbf{x} - \mathbf{y}|} + \frac{[(\mathbf{y} - \mathbf{x}) \cdot \mathbf{e}_i][(\mathbf{y} - \mathbf{x}) \cdot \mathbf{e}_j]}{|\mathbf{x} - \mathbf{y}|^3}, \tag{16}$$

$$T_{ijk}(\mathbf{y}, \mathbf{x}) = -\frac{6[(\mathbf{y} - \mathbf{x}) \cdot \mathbf{e}_i][(\mathbf{y} - \mathbf{x}) \cdot \mathbf{e}_j][(\mathbf{y} - \mathbf{x}) \cdot \mathbf{e}_k]}{|\mathbf{x} - \mathbf{y}|^5}. \tag{17}$$

Note that G_{ij} and T_{ijk} are actually the Cartesian components of the free-space second-rank Oseen-Burgers Green tensor \mathbf{G} and associated third-rank stress tensor \mathbf{T} . The identity (15) shows that when computing the velocity \mathbf{u} about the particle it is actually sufficient to know two vectors on the particle surface: the velocity \mathbf{u} and the surface traction $\mathbf{f} = \boldsymbol{\sigma} \cdot \mathbf{n}$. In getting these quantities it is necessary to let the point \mathbf{x} in (15) tend onto the surface S . This is adequately achieved by appealing to the key identity

$$\int_S T_{ijk}(\mathbf{y}, \mathbf{x}) n_k(\mathbf{y}) dS(\mathbf{y}) = 0 \quad \text{for } \mathbf{x} \text{ in } \mathcal{D}. \quad (18)$$

Setting $\mathbf{u} = u_j \mathbf{e}_j$ and combining (15) with (18) one then arrives at the equivalent and fruitful velocity integral representation

$$\begin{aligned} 8\pi u_j(\mathbf{x}) &= \int_S [u_i(\mathbf{y}) - u_i(\mathbf{x})] T_{ijk}(\mathbf{y}, \mathbf{x}) n_k(\mathbf{y}) dS(\mathbf{y}) \\ &\quad - \frac{1}{\mu} \int_S [\mathbf{e}_i \cdot \boldsymbol{\sigma} \cdot \mathbf{n}](\mathbf{y}) G_{ij}(\mathbf{y}, \mathbf{x}) dS(\mathbf{y}) \quad \text{for } \mathbf{x} \text{ in } \mathcal{D}. \end{aligned} \quad (19)$$

3.2 Relevant boundary-integral equation

By virtue of the Navier boundary condition (3), it turns out that it is sufficient in gaining both the velocity \mathbf{u} and the traction $\mathbf{f} = \boldsymbol{\sigma} \cdot \mathbf{n}$ on the surface S to introduce the unknown quantity d and vector \mathbf{d} tangent to S such that

$$d = \mathbf{n} \cdot \boldsymbol{\sigma} \cdot \mathbf{n} / \mu, \quad \mathbf{d} = [\boldsymbol{\sigma} \cdot \mathbf{n} - (\mathbf{n} \cdot \boldsymbol{\sigma} \cdot \mathbf{n}) \mathbf{n}] / \mu = d_i \mathbf{e}_i. \quad (20)$$

Note that by definition $\mathbf{d} \cdot \mathbf{n} = 0$. Inspecting the definitions (16)-(17) furthermore shows that (19) also holds for \mathbf{x} on the particle surface S ! Injecting the Navier boundary condition (3) in (19) and letting \mathbf{x} tend onto the surface S then immediately provides the following problem for the unknown surface quantities (d, \mathbf{d})

$$L_i[d, \mathbf{d}] = [\mathbf{U} + \boldsymbol{\Omega} \wedge \mathbf{OM}] \cdot \mathbf{e}_i \quad \text{for } \mathbf{x} \text{ on } S (i = 1, 2, 3), \quad (21)$$

$$\mathbf{d} \cdot \mathbf{n} = 0 \quad \text{for } \mathbf{x} \text{ on } S \quad (22)$$

where the coupled and *regularized* Fredholm boundary-integral equations of the second kind (21) have linear operators L_i defined by the identity

$$\begin{aligned} 8\pi L_i[d, \mathbf{d}] &= -8\pi \lambda d_i(\mathbf{x}) - \int_S G_{ki}(\mathbf{y}, \mathbf{x}) d_k(\mathbf{y}) dS(\mathbf{y}) \\ &\quad - \int_S G_{ki}(\mathbf{y}, \mathbf{x}) n_k(\mathbf{y}) d(\mathbf{y}) dS(\mathbf{y}) \\ &\quad + \lambda \int_S [d_k(\mathbf{y}) - d_k(\mathbf{x})] T_{kil}(\mathbf{y}, \mathbf{x}) n_l(\mathbf{y}) dS(\mathbf{y}). \end{aligned} \quad (23)$$

Of course, for $\lambda = 0$ the definitions (20) and the problem (21)-(22) reduce to the well-known boundary-integral equation

$$\begin{aligned}
 & -\frac{1}{8\pi\mu} \int_S G_{ki}(\mathbf{y}, \mathbf{x}) [\mathbf{f} \cdot \mathbf{e}_k](\mathbf{y}) dS(\mathbf{y}) \\
 & = [\mathbf{U} + \boldsymbol{\Omega} \wedge \mathbf{OM}] \cdot \mathbf{e}_i \text{ for } \mathbf{x} \text{ on } S
 \end{aligned} \tag{24}$$

which governs (see Pozrikidis (1992)) the surface traction \mathbf{f} exerted on the boundary of a no-slip particle experiencing the rigid-body motion $(\mathbf{U}, \boldsymbol{\Omega})$.

In summary, for a slip particle one has to invert boundary-integral equations (21) in conjunction with the property $\mathbf{d} \cdot \mathbf{n} = 0$ (recalled by (22)). Once this is done, the knowledge of (d, \mathbf{d}) permits one to get on the particle surface not only both vectors $\mathbf{f} = \mu(d\mathbf{n} + \mathbf{d})$ and \mathbf{u} (and therefore also the resulting net force \mathbf{F} and net torque \mathbf{L} experienced by the migrating particle) but also, whenever needed, the velocity field \mathbf{u} at any arbitrary point in the liquid domain \mathcal{D} by either appealing to the integral representation (15) or (19). In getting the resistance tensors $\mathbf{A}, \mathbf{B} = {}^t\mathbf{C}$ and \mathbf{D} one has to solve six times (21)-(22) successively for $(\mathbf{U}, \boldsymbol{\Omega}) = (\mathbf{e}_i, \mathbf{0})$ and $(\mathbf{U}, \boldsymbol{\Omega}) = (\mathbf{0}, \mathbf{e}_i)$ (with $i = 1, 2, 3$).

4 Numerical implementation and results

This section briefly presents the implemented boundary element technique employed to numerically invert the problem (21)-(22). It also benchmarks the method against analytical results for a sphere and numerical results obtained elsewhere for spheroids. Finally, it reports numerical results for a few non-axisymmetric and orthotropic particles.

4.1 Numerical strategy

Each boundary-integral equation (21) is numerically discretized and inverted by employing boundary elements and a collocation point method (see C. A. Brebbia and Wrobel (1984); Beskos (1998); Bonnet (1999)). More precisely, we appeal on the particle surface S to a N -node mesh consisting, for a sake of accuracy, of 6-node curvilinear and triangular boundary elements (as in Sellier and Pasol (2006); Sellier (2007, 2008)). At each nodal point it is possible to introduce from the knowledge (exact or computed value) of the unit outward normal \mathbf{n} two additional unit vectors \mathbf{t}_1 and \mathbf{t}_2 tangent to the particule surface S and obeying the property $\mathbf{t}_1 \cdot \mathbf{t}_2 = 0$. From its definition (20) the vector \mathbf{d} is tangent to the particle surface S and therefore writes $\mathbf{d} = d_1^t \mathbf{t}_1 + d_2^t \mathbf{t}_2$. Hence, at each nodal point one ends up with three unknown quantities in solving (21)-(22): the normal component d and the tangential components d_1^t and d_2^t of the vector \mathbf{f}/μ . For a given N -node mesh we thus

have $3N$ unknown values (d, d_1^l, d_2^l) . Those quantities satisfy a $3N$ -equation linear system obtained by discretizing the coupled boundary-integral equations (21) and using the relation $d_k = d_1^l \mathbf{t}_1 \cdot \mathbf{e}_k + d_2^l \mathbf{t}_2 \cdot \mathbf{e}_k$ for each encountered Cartesian component d_k . In summary, once discretized the problem (21)-(22) yields a linear system $AX = Y$ with $3N \times 3N$, non-symmetric and fully-populated so-called influence square matrix A . Accurately computing the entries of the dense matrix A is a key and challenging task. The employed procedure makes use of local polar coordinates to remove on a boundary element the weakly-singular contributions encountered when the nodal point at which (21) is numerically enforced belongs to this element. For further details regarding this issue the reader is directed to Sellier (2011). Finally, the system $AX = Y$ is solved by Gaussian elimination.

4.2 Numerical comparisons and results for orthotropic slip particles

Although the proposed method holds whatever the particle smooth shape, we henceforth present numerical comparisons and results for orthotropic slip particles. By definition a particle is orthotropic when it has three normal planes of symmetry intersecting at its center of volume O . Here we select our Cartesian coordinates (O, x_1, x_2, x_3) such that the orthotropic particle's planes of symmetry are normal to the vectors $\mathbf{e}_1, \mathbf{e}_2$ and \mathbf{e}_3 . Under these choices, symmetry considerations easily show that, for a slip orthotropic particle with length scale a , the exerted net hydrodynamic force \mathbf{F} and torque \mathbf{L} about the center of volume O satisfy (remind (4) and (5))

$$\mathbf{F} = -6\pi\mu a f_i \mathbf{U} \quad \text{and} \quad \mathbf{L} = \mathbf{0} \quad \text{for} \quad \mathbf{U} \wedge \mathbf{e}_i = \boldsymbol{\Omega} = \mathbf{0}, \quad (25)$$

$$\mathbf{L} = -8\pi\mu a^3 c_i \boldsymbol{\Omega} \quad \text{and} \quad \mathbf{F} = \mathbf{0} \quad \text{for} \quad \boldsymbol{\Omega} \wedge \mathbf{e}_i = \mathbf{U} = \mathbf{0} \quad (26)$$

where the occurring (dimensionless) force friction coefficients f_1, f_2, f_3 and torque friction coefficient c_1, c_2 and c_3 depend upon the particle geometry and normalized slip length $\lambda/a \geq 0$. Comparing (25)-(26) with (5) thus shows that for a slip orthotropic particle both transposed resistance coupling tensors \mathbf{C} and \mathbf{D} vanish whereas the resistance tensors \mathbf{A} and \mathbf{B} are diagonal with Cartesian components A_{ij} and D_{ij} given by the relations

$$A_{ij} = 6\pi a \delta_{ij} f_i, \quad D_{ij} = 8\pi a^3 \delta_{ij} c_i. \quad (27)$$

4.2.1 Numerical comparisons for slip spherical or spheroidal particles

As mentioned in the introduction, the previous friction coefficients have been either analytically or numerically obtained in the literature for spherical and spheroidal slip particles. For a sphere with radius a inspecting (11) and (14) gives $f_1 = f_2 =$

Table 1: Computed friction coefficients $f_1 = f_2 = f_3$ and $c_1 = c_2 = c_3$ for a slip sphere with radius a versus the number N of nodal points and for $\lambda/a = 0.5, 2$.

	λ/a	$N = 74$	$N = 242$	$N = 1058$	analytical
f_i	0.5	0.80287	0.80018	0.80001	0.8
c_i	0.5	0.39817	0.39988	0.39999	0.4
f_i	2	0.72045	0.71483	0.71433	0.71429
c_i	2	0.14188	0.14278	0.14285	0.14286

$f_3 = c_{\text{sphere}}$ and $c_1 = c_2 = c_3 = c_{\text{sphere}}$ with $f_{\text{sphere}} = (1 + 2\lambda/a)c_{\text{sphere}}$ and $c_{\text{sphere}} = (1 + 3\lambda/a)^{-1}$.

As seen in Table 1, our numerical computations nicely retrieve those analytical results as the number N of nodal points spread on the sphere boundary increases.

Additional comparisons for the force and torque friction coefficients f_i and c_i have been achieved for slip spheroids. More precisely, we select a spheroidal particle with center O and surface S having the equation $(x_1/a)^2 + (x_2/a)^2 + (x_3/b)^2 = 1$. Comparisons for the force friction coefficients $f_1 = f_2$ and f_3 against the results obtained in Keh and Chang (2008) and in Chang and Keh (2011) by quite different approaches are reported in Table 2 both for prolate ($b/a = 2$) and oblate ($b/a = 0.5$) spheroids and normalized slip length $\lambda/a = 0.5, 2$. Clearly, the computed values of f_1 and f_3 perfectly agree with the ones obtained in previous works.

In a similar fashion, comparisons for the torque friction coefficients $c_1 = c_2$ and c_3 are displayed in Table 3. One should note that the results reported in Chang and Keh (2009) are not exact since obtained by considering the spheroid as a small perturbation of a spherical shape. Actually, both results obtained by retaining the first-order and the second-order approximations are given in Chang and Keh (2009) and we only report in our Table 3 the ones predicted by the second-order approximation. As seen in Table 3, our results are in very good agreement both with Chang and Keh (2009) and Loyalka and Griffin (1994) for the torque friction coefficient c_3 . By contrast, small differences are found for the coefficient c_1 . We believe the results given for c_1 in Chang and Keh (2009) to be not accurate enough because the values found for the coefficient c_1 (but not for the coefficient c_3) in Chang and Keh (2009) by the first-order and the second-order approximations are slightly different. This reveals a slow convergence of the employed asymptotic procedure for the evaluation of c_1 and clearly suggests that higher-order approximations are needed in calculating such a coefficient.

4.2.2 Numerical results for slip ellipsoids and an open torus

This section illustrates the sensitivity of the friction coefficients f_i and c_i to the shape of a slip particle by comparing these coefficients for several *volume equivalent* slip orthotropic particles: a sphere with radius a , an open torus and two non-spheroidal ellipsoids.

The selected open torus has axis of revolution (O, \mathbf{e}_3) , circular cross-section with radius R and hole radius R . Since its volume $4\pi^2 R^3$ is the same as the sphere volume $4\pi a^3/3$ one gets $R = a(3\pi)^{-1/3} \sim 0.4734a$. Because the torus is axisymmetric $f_1 = f_2$ and $c_1 = c_2$. Convergence of the computed friction coefficients f_1, f_3, c_1 and c_3 versus the number N of nodal points spread on the torus boundary is examined in Table 4 for $\lambda/a = 0, 2.5, 5$. For comparisons, the results obtained for the no-slip ($\lambda = 0$) torus in Majumdar and O’Neill (1977) and Goren and O’Neill (1980) are also reported in Table 4 caption.

It turns out that putting 1152 nodal points on the torus boundary permits one to accurately compute the torus friction coefficient in the entire range $\lambda/a \leq 5$. In order to illustrate the ability of the procedure to cope with non-axisymmetric slip particles we also consider slip ellipsoids with surface admitting the equation $(x_1/a)^2 + \beta^2(x_2/a)^2 + (x_3/\beta a)^2 = 1$, where for symmetry reasons, it is sufficient to confine attention to $\beta > 1$ (one has to switch the values of f_2 and f_3 and the values of c_2 and c_3 when $\beta > 0$ is replaced with $1/\beta$). Here we report results for $\beta = 3/2, 2$. Computed values of the friction coefficients are displayed versus the

Table 2: Computed force friction coefficients $f_1 = f_2$ and f_3 for a spheroidal particle with $\lambda/a = 0.1, 1$ using N_1, N_2 or N_3 collocation points on the particle surface. Here $N_1 = 74, N_2 = 242$ and $N_3 = 1058$ for the oblate spheroid ($b/a = 0.5$) and $N_1 = 170, N_2 = 530$ and $N_3 = 2210$ for the prolate spheroid ($b/a = 2$). The last column in the Table indicates the value obtained in the literature by Keh and Chang (2008) or Chang and Keh (2011).

	λ/a	b/a	N_1	N_2	N_3	literature
f_1	0.1	0.5	0.7131	0.7144	0.7143	0.7142
f_3	0.1	0.5	0.8479	0.8453	0.8448	0.8448
f_1	1	0.5	0.5444	0.5416	0.5403	0.5402
f_3	1	0.5	0.7748	0.7704	0.7696	0.7696
f_1	0.1	2	1.3003	1.2994	1.2994	1.2994
f_3	0.1	2	1.1153	1.1162	1.1163	1.1163
f_1	1	2	1.1254	1.1234	1.1233	1.1233
f_3	1	2	0.8159	0.8142	0.8141	0.8141

Table 3: Computed torque friction coefficients $c_1 = c_2$ and c_3 for a spheroidal particle using N_1, N_2 or N_3 collocation points on the particle surface. Again, $N_1 = 74, N_2 = 242$ and $N_3 = 1058$ for the oblate spheroid ($b/a = 0.5$) and $N_1 = 170, N_2 = 530$ and $N_3 = 2210$ for the prolate spheroid ($b/a = 2$). The last column in the Table indicates the value obtained in the literature by Chang and Keh (2009) and for the last two lines by Loyalka and Griffin (1994).

	λ/a	b/a	N_1	N_2	N_3	literature
c_1	0.1	0.5	0.4412	0.4364	0.4357	0.4423
c_3	0.1	0.5	0.5254	0.5235	0.5233	0.5231
c_1	1	0.5	0.2350	0.2285	0.2276	0.2353
c_3	1	0.5	0.1596	0.1595	0.1595	0.1584
c_1	0.1	2	2.5278	2.5278	2.5279	2.4436
c_3	0.1	2	1.2750	1.2742	1.2741	1.2757
c_1	1	2	1.3803	1.3785	1.3784	1.3161
c_3	1	2	0.4422	0.4426	0.4426	0.4460
c_3	0.05	0.5	0.6029	0.6005	0.6003	0.6004
c_3	0.2	2	1.0538	1.0535	1.0535	1.0535

number of nodal points in Table 5 again for $\lambda/a = 0, 2.5, 5$.

Clearly, taking this time 434 or 530 nodes on the ellipsoid surface is quite sufficient to obtain very accurate results for $\beta = 3/2$ or $\beta = 2$, respectively. Henceforth, we put for computations $N = 1152$ nodes on the torus, $N = 1634$ nodes on the $\beta = 3/2$ ellipsoid and $N = 2210$ nodes on the $\beta = 2$ ellipsoid. The sensitivity of each force friction f_i coefficient to the particle shape is then illustrated in Fig. 2-4.

Not surprisingly, each force friction coefficient is seen to decay as the slip length increases because the flow slips more on the particle surface. The coefficient f_i strongly depends upon both the particle's direction of translation (value of i) and the particle's shape (sphere, open torus or ellipsoid). For f_1 and f_2 there is a clear hierarchy (i. e. no crossing curves in Fig 2 and Fig 3) which however is not the same for f_1 and f_2 (curves for the open torus and the $\beta = 3/2$ ellipsoid switch ranks). In contrast, curves for the two ellipsoids intersect for f_3 (see Fig. 4) at $\lambda/a \sim 0.5$. When subject to a gravity field $\mathbf{g} = g\mathbf{e}_i$ (i. e. aligned with the direction \mathbf{e}_i) each particle settles parallel with \mathbf{e}_i with, for particles having the same uniform density ρ_s , velocity $(f_{sphere}/f_i)\mathbf{U}_{sphere}$ where f_{sphere} is the friction coefficient for the sphere and $\mathbf{U}_{sphere} = 2a^2(\rho_s - \rho)\mathbf{g}/(9\mu f_{sphere})$. For instance, Fig. 2 and Fig. 3 reveal that the slip sphere settles faster in the \mathbf{e}_1 and \mathbf{e}_2 directions than the volume-equivalent slip open torus or the considered ellipsoids (all having the same slip length as the sphere).

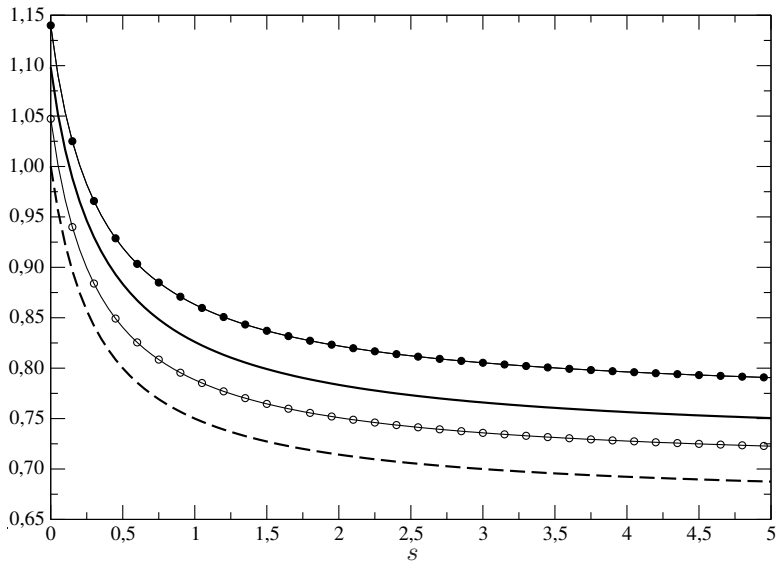


Figure 2: Force friction coefficients f_1 versus $s = \lambda/a$ for a slip sphere (dashed line), a slip open torus (solid line), a slip ellipsoid with $\beta = 3/2$ (○ symbols) and a slip ellipsoid with $\beta = 2$ (● symbols).

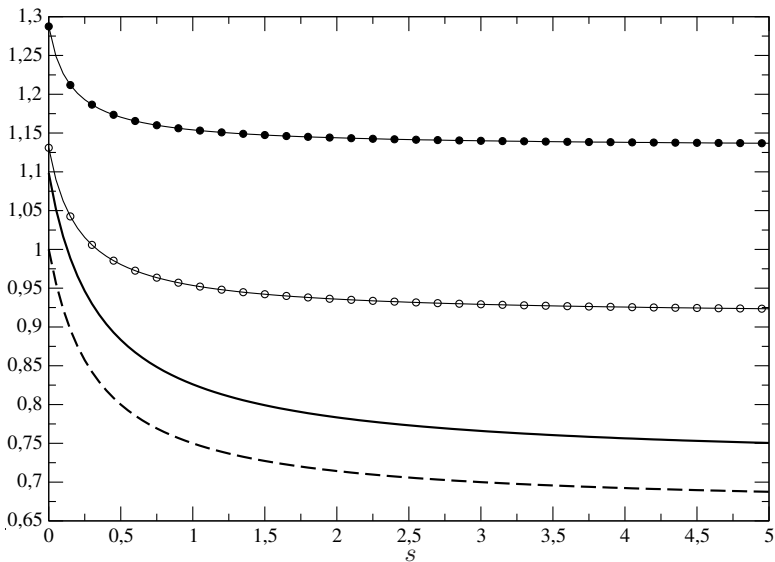


Figure 3: Force friction coefficients f_2 versus $s = \lambda/a$ for a slip sphere (dashed line), a slip open torus (solid line), a slip ellipsoid with $\beta = 3/2$ (○ symbols) and a slip ellipsoid with $\beta = 2$ (● symbols).

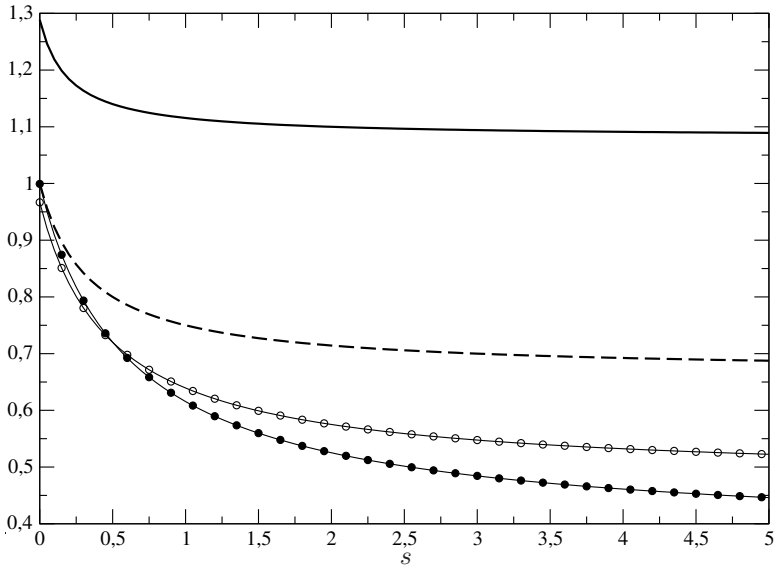


Figure 4: Force friction coefficients f_3 versus $s = \lambda/a$ for a slip sphere (dashed line), a slip open torus (solid line), a slip ellipsoid with $\beta = 3/2$ (\circ symbols) and a slip ellipsoid with $\beta = 2$ (\bullet symbols).

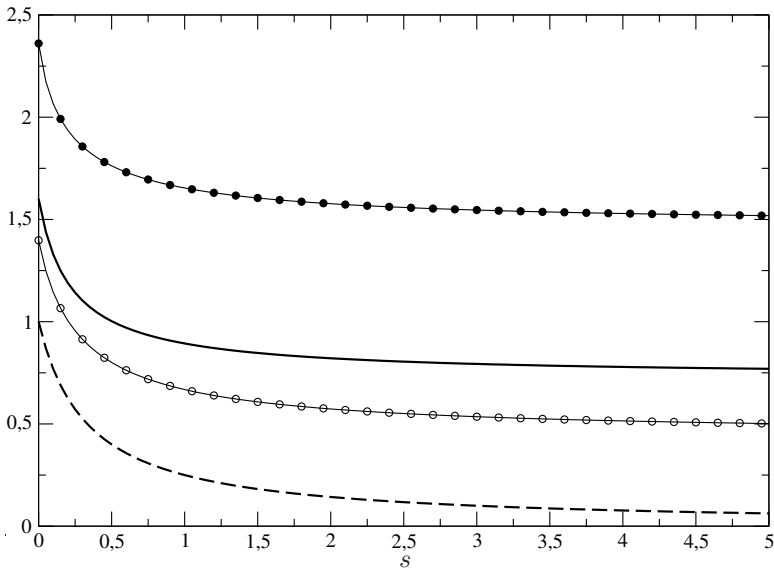


Figure 5: Torque friction coefficients c_1 versus $s = \lambda/a$ for a slip sphere (dashed line), a slip open torus (solid line), a slip ellipsoid with $\beta = 3/2$ (\circ symbols) and a slip ellipsoid with $\beta = 2$ (\bullet symbols).

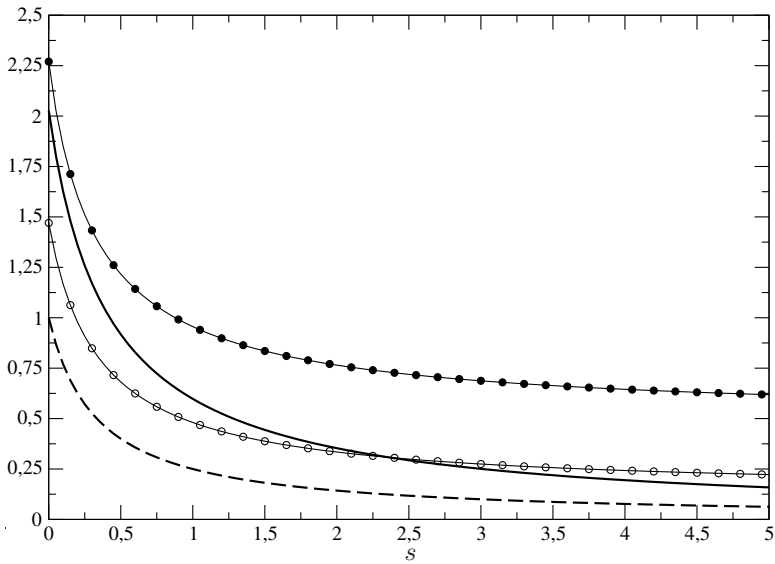


Figure 6: Torque friction coefficients c_2 versus $s = \lambda/a$ for a slip sphere (dashed line), a slip open torus (solid line), a slip ellipsoid with $\beta = 3/2$ (\circ symbols) and a slip ellipsoid with $\beta = 2$ (\bullet symbols).

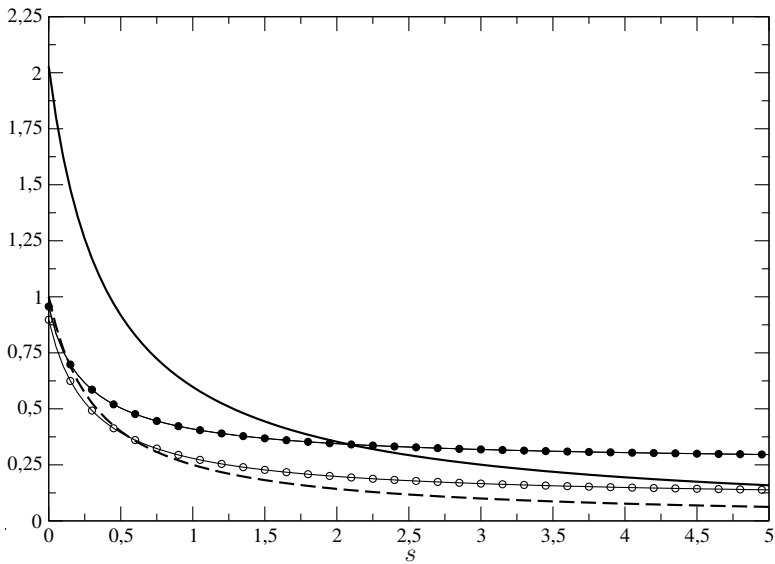


Figure 7: Torque friction coefficients c_3 versus $s = \lambda/a$ for a slip sphere (dashed line), a slip open torus (solid line), a slip ellipsoid with $\beta = 3/2$ (\circ symbols) and a slip ellipsoid with $\beta = 2$ (\bullet symbols).

Table 4: Computed torque friction coefficients $f_1 = f_2, f_3, c_1 = c_2$ and c_3 for a slip open torus for $\lambda/a = 0, 2.5, 5$ putting $N_1 = 288, N_2 = 1152$ or $N_3 = 4608$ collocation points on the torus surface. For $\lambda = 0$ the results given in Majumdar and O’Neill (1977) and Goren and O’Neill (1980) are $f_1 = f_2 = 1,0983, f_3 = 1,2884, c_1 = c_2 = 1,6014$ and $c_3 = 2,0277$.

	λ/a	N_1	N_2	N_3
f_1	0	1.0976	1.0984	1.0983
f_3	0	1.2886	1.2885	1.2884
c_1	0	1.6037	1.6016	1.6015
c_3	0	2.0279	2.0277	2.0278
f_1	2.5	0.7805	0.7732	0.7726
f_3	2.5	1.0990	1.0965	1.0963
c_1	2.5	0.8071	0.8048	0.8046
c_3	2.5	0.2928	0.2933	0.2934
f_1	5	0.7587	0.7505	0.7498
f_3	5	1.0918	1.0892	1.0890
c_1	5	0.7722	0.7697	0.7694
c_3	5	0.1586	0.1589	0.1589

In a similar fashion, attention is paid to the torque friction coefficients f_i in Fig. 5-7. These coefficients decay as λ increases and the larger decay rate is obtained for the slip sphere whatever the addressed coefficient c_i . Clearly, the particles hierarchy strongly depends upon the direction of rotation (selected value of i) for $s = \lambda/a \leq 5$. This time two of the retained volume-equivalent slip particles admit the same torque friction coefficient c_2 or c_3 for specific values of the normalized slip λ/a .

5 Conclusions

A new boundary approach has been proposed to accurately compute the surface traction and resulting net hydrodynamic force and torque exerted on a solid and arbitrarily-shaped slip particle experiencing a prescribed rigid-body motion in a quiescent Newtonian liquid. The procedure assumes that the flow about the particle is a creeping flow which satisfies on the particle surface the Navier slip condition and requires in general to solve six boundary-integral equations (on the particle boundary) associated with the degrees of freedom of the particle’s rigid-body motion). Such a task is achieved in the present paper by implementing a boundary element technique which yields very accurate results as demonstrated by convincing comparisons against analytical results for a slip sphere and numerical results obtained for slip spheroidal particles by previous authors using quite different meth-

Table 5: Computed torque friction coefficients f_i and c_i for a slip ellipsoid and $\lambda/a = 0, 2.5, 5$ using $N_1 = 122, N_2 = 434$ or $N_3 = 1634$ collocation points for $\beta = 3/2$ and $N_1 = 170, N_2 = 530$ or $N_3 = 2210$ collocation points $\beta = 2$.

	λ/a	β	N_1	N_2	N_3
f_1	0	3/2	1.0478	1.0473	1.0473
f_2	0	3/2	1.1319	1.1310	1.1310
f_3	0	3/2	0.9658	0.9667	0.9667
c_1	0	3/2	1.3972	1.3978	1.3980
c_2	0	3/2	1.4711	1.4704	1.4704
c_3	0	3/2	0.9005	0.8978	0.8976
f_1	2.5	3/2	0.7456	0.7420	0.7421
f_2	2.5	3/2	0.9349	0.9318	0.9319
f_3	2.5	3/2	0.5648	0.5594	0.5591
c_1	2.5	3/2	0.5533	0.5509	0.5510
c_2	2.5	3/2	0.2999	0.2994	0.2993
c_3	2.5	3/2	0.1847	0.1797	0.1795
f_1	5	3/2	0.7268	0.7233	0.7226
f_2	5	3/2	0.9265	0.9234	0.9235
f_3	5	3/2	0.5296	0.5230	0.5226
c_1	5	3/2	0.5045	0.5019	0.5020
c_2	5	3/2	0.2234	0.2227	0.2225
c_3	5	3/2	0.1437	0.1387	0.1385
f_1	0	2	1.1388	1.1401	1.1400
f_2	0	2	1.2887	1.2874	1.2875
f_3	0	2	0.9982	0.9992	0.9993
c_1	0	2	2.3587	2.3598	2.3606
c_2	0	2	2.2701	2.2702	2.2701
c_3	0	2	0.9612	0.9572	0.9568
f_1	2.5	2	0.8087	0.8133	0.8123
f_2	2.5	2	1.1470	1.1415	1.1416
f_3	2.5	2	0.5053	0.5019	0.5016
c_1	2.5	2	1.5698	1.5577	1.5588
c_2	2.5	2	0.7168	0.7201	0.7194
c_3	2.5	2	0.3470	0.3301	0.3294
f_1	5	2	0.7877	0.7918	0.7906
f_2	5	2	1.1424	1.1367	1.1368
f_3	5	2	0.4513	0.4466	0.4461
c_1	5	2	1.5298	1.5175	1.5186
c_2	5	2	0.6162	0.6194	0.6186
c_3	5	2	0.3138	0.2968	0.2961

ods. New numerical results given for volume equivalent torus and non-spheroidal ellipsoids highlight the sensibility of a particle friction coefficients to the particle slip length and geometry.

For some basic applications the slip particle is subject to a prescribed ambient and arbitrary (for instance, not uniform) Stokes flow. Determining the resulting particle rigid-body migration is then a key but difficult task. For a slip sphere ($\lambda > 0$) it has been fortunately possible in Keh and Chen (1996) to analytically get the sphere's translational and angular velocities by nicely extending the famous relations established by Faxen (1922-1923) when there is no slip ($\lambda = 0$) over the sphere surface. However, no analogous results are currently available for non-spherical slip particles although the migration of a slip particle in a given ambient flow is clearly expected to depend upon the particle shape. Investigations regarding this challenging issue require additional efforts and are therefore postponed to another work.

References

- Basset, A. B.** (1961): *A treatise on Hydrodynamics*. Vol. 2. Dover, New York, 1961.
- Baudry, J.; Charlaix, E.; Tonck, A.; Mazuyer, D.** (2001): Experimental evidence for a large slip effect at a nonwetting fluid-solid interface. *Langmuir*, vol. 17, pp. 5232–5236.
- Beskos, D. E.** (1998): *Introduction to Boundary Element Methods*. Elsevier Science Publishers.
- Bonnet, M.** (1999): *Boundary Integral Equation Methods for Solids and Fluids*. John Wiley & Sons Ltd.
- C. A. Brebbia, J. C. T.; Wrobel, L. C.** (1984): *Boundary Element Techniques*. Springer-Verlag, Theory and Applications in Engineering, Berlin Heidelberg New York Tokyo.
- Chang, Y. C.; Keh, H. J.** (2009): Translation and rotation of slightly deformed colloidal spheres experiencing slip. *Journal of Colloid and Interface Science*, vol. 330, pp. 201–210.
- Chang, Y. C.; Keh, H. J.** (2011): Theoretical study of the creeping motion of axially and fore-and-aft symmetric slip particles in an arbitrary directions. *European Journal of Mechanics B/Fluids*, vol. 30, pp. 236–244.
- Churaev, N.; Sobolev, V.; Somov, A. N.** (1994): Slippage of liquids over lyophobic solid surfaces. *J. Colloid Int. Sci.*, vol. 97, pp. 574–581.
- Deo, S.; Datta, S.** (1996): Slip flow past a prolate spheroid. *Indian J. Pure Appl. Math.*, vol. 33, pp. 903–909.

- Faxen, H.** (1922-1923): Die Bewegung einer starren Kugel langs der Achse eines mit zaeher Fluessigkeit gefuellten Rohres. *Arkiv for Matematik, Astronomi och Fysik*, vol. 17, no. 27, pp. 1–28.
- Goren, S. L.; O’Neill, M. E.** (1980): Axisymmetric creeping motion of an open torus. *J. Fluid Mech.*, vol. 101, pp. 97–110.
- Happel, J.; Brenner, H.** (1991): *Low Reynolds number hydrodynamics*. Kluwer Academic Publishers, Dordrecht, Boston, London.
- Jeffery, G. B.** (1922): The motion of ellipsoidal particles immersed in a viscous fluid. *Proc. Roy. Soc. A.*, vol. 102, pp. 161–179.
- Keh, H. J.; Chang, Y. C.** (2008): Slow motion of a slip spheroid along its axis of revolution. *International Journal of Multiphase Flow*, vol. 34, pp. 713–722.
- Keh, H. J.; Chen, S. H.** (1996): The motion of a slip spherical particle in an arbitrary stokes flow. *European Journal of Mechanics B/Fluids*, vol. 15, pp. 791–807.
- Keh, H. J.; Huang, C. C.** (2004): Slow motion of axisymmetric slip particles along their axes of revolution. *International Journal of Engineering Science*, vol. 42, pp. 1621–1644.
- Kim, S.; Karrila, S.** (1991): *Microhydrodynamics: Principles and Selected Applications*. Butterworth-Heinemann.
- Lamb, H.** (1932): *Hydrodynamics*. 6th edn. Cambridge University Press, 1932.
- Loyalka, S. K.** (1996): Rotation of a closed torus in the slip regime. *J. Aerosol. Sci.*, vol. 25, pp. 371–379.
- Loyalka, S. K.; Griffin, J. L.** (1994): Rotation of non-spherical axi-symmetric particles in the slip regime. *J. Aerosol. Sci.*, vol. 25, pp. 509–525.
- Majumdar, S. R.; O’Neill, M. E.** (1977): On axisymmetric stokes flow past a torus. *Z. Angew. Math. Phys.*, vol. 28, pp. 541–550.
- Navier, C. L. M. H.** (1823): Mémoire sur les lois du mouvement des fluides. *Mémoire de l’Académie Royale des Sciences de l’Institut de France*, vol. 6, pp. 389–440.
- Palaniappan, D.** (1994): Creeping flow about a slightly deformed sphere. *Z. Angew. Math. Phys.*, vol. 45, pp. 832–838.
- Pozrikidis, C.** (1992): *Boundary integral and singularity methods for linearized viscous flow*. Cambridge University Press.
- Ramkissoon, H.** (1997): Slip flow past an approximate spheroid. *Acta Mech.*, vol. 123, pp. 227–233.

Sellier, A. (2007): Slow viscous migration of a conducting solid particle under the action of uniform ambient electric and magnetic fields. *CMES: Computer Modeling in Engineering & Sciences*, vol. 21, no. 2, pp. 105–132.

Sellier, A. (2008): Slow viscous motion of a solid particle in a spherical cavity. *CMES: Computer Modeling in Engineering & Sciences*, vol. 25, no. 3, pp. 165–179.

Sellier, A. (2011): Boundary element technique for slow viscous flows about particles. In Aliabadi, M.; Wen, P. H.(Eds): *In boundary Element Methods in Engineering And Sciences*. Imperial College Press.

Sellier, A.; Pasol, L. (2006): Sedimentation of a solid particle immersed in a fluid film. *CMES: Computer Modeling in Engineering & Sciences*, vol. 16, no. 3, pp. 187–196.

Senchenko, S.; Keh, H. J. (2006): Slipping stokes flow around a slightly deformed sphere. *Acta Mech.*, vol. 18, pp. 088104.

Williams, M. M. R. (1987): A closed torus in stokes flow with slip boundary condition. *Q. J. Mech. Appl. Math.*, vol. 40, pp. 235–243.

Williams, M. M. R. (1987): Neutron diffusion in spheroidal, bispherical and toroidal systems. *Nucl. Sci. and Engr.*, vol. 94, pp. 251–263.

Williams, M. M. R.; Loyalka, S. K. (1991): *Aerosol Science: Theory and Practice with Special Applications to Nuclear Industry*. Pergamon, Oxford, 1991.